Development and optical testing of the camera, hand lens, and microscope probe with scannable laser spectroscopy (CHAMP-SLS)

Greg S. Mungas[*a], Yekta Gürsel[a], Cesar A. Sepulveda[a], Mark Anderson[a],
Clayton La Baw[a], Kenneth R. Johnson[a], Matthew Deans[b], Luther Beegle[a], John Boynton[a]
[a]Jet Propulsion Laboratory, Caltech, 4800 Oak Grove Dr. Pasadena, CA 91109
[b]NASA Ames Research Center, MS 269-3, Moffett Field, CA 94035

ABSTRACT

Conducting high resolution field microscopy with coupled laser spectroscopy that can be used to selectively analyze the surface chemistry of individual pixels in a scene is an enabling capability for next generation robotic and manned spaceflight missions, civil, and military applications. In the laboratory, we use a range of imaging and surface preparation tools that provide us with in-focus images, context imaging for identifying features that we want to investigate at high magnification, and surface-optical coupling that allows us to apply optical spectroscopic analysis techniques for analyzing surface chemistry particularly at high magnifications. The camera, handlens, and microscope probe with scannable laser spectroscopy (CHAMP-SLS) is an imaging/spectroscopy instrument capable of imaging continuously from infinity down to high resolution microscopy (resolution of ~1 micron/pixel in a final camera format), the closer CHAMP-SLS is placed to a feature, the higher the resultant magnification. At hand lens to microscopic magnifications, the imaged scene can be selectively interrogated with point spectroscopic techniques such as Raman spectroscopy, microscopic Laser Induced Breakdown Spectroscopy (micro-LIBS), laser ablation mass-spectrometry, Fluorescence spectroscopy, and/or Reflectance spectroscopy. This paper summarizes the optical design, development, and testing of the CHAMP-SLS optics.

Keywords: Camera, hand lens, microscope, microscopy, spectroscopy, Raman, micro-LIBS, Fluorescence, laser ablation, mass-spectrometry

1. INTRODUCTION

The invention for imaging continuously from infinity down to microscopy in visible wavelengths was originally developed in 1998-2001 under NASA's Mars Instrument Development Program (MIDP) [1]. This instrument was designated as the original MIDP CHAMP and provides infinity down to ~3 micron per pixel imaging resolution in the 450nm-650nm spectral range where the imaging performance is essentially achromatic. Every working distance from 5mm to infinity has a corresponding best-focus solution between the two lens cells that make up the MIDP CHAMP optical design, the closer the instrument is placed to a target, the higher the imaging resolution at the cost of a correspondingly smaller field-of-view (see Figure 1). The original MIDP CHAMP optical design process involved over 1000's of design iterations utilizing Zemax optical design, analysis, and optimization software to find local optimum candidate design solutions in a very large optical design space that was at the time perceived to be heavily optically constrained. The MIDP CHAMP instrument provided a 8 to 10-fold improvement in field microscopic resolution from a robotic arm compared to what is currently being flown on the Mars Exploration Rover and Mars Phoenix missions. MIDP CHAMP's resolution is higher than Phoenix's and Beegle's fixed microscopes both at 4 micron/pixel [2,3,4,5].

Two important attributes in conducting field microscopy from a remote platform derived from the MIDP CHAMP work were: 1) the ability to progressively image at higher magnifications through the instrument directly in order to provide the context imaging and instrument positioning accuracy necessary for placing a high magnification/small field-of-view on a microscopic target feature of interest, and 2) the ability to acquire image slices at depth-of-field spacing in order to ultimately provide in-focus topographic images of surfaces that have inherent roughness greater than the imaging system's depth-of-field[†]. Attribute (1) is important for ultimately helping to remove arm inaccuracies associated with actuator backlash and compliant structures that deviate from ideal rigid behavior particularly when

[*] Greg.Mungas@jpl.nasa.gov; phone: 626-755-8819;
[†] In a laboratory, flat and/or polished sample slides are carefully prepared in order to remain within the depth-of-field limits of high magnification microscopes. This luxury doesn't readily exist with field deployed microscopes.

using arm placement sensors that do not directly provide relative positioning vectors to the target of interest. Furthermore, for high magnification instruments with short working distances, these sensors are commonly occluded by the instruments that they are trying to emplace. Attribute (2) allows one to conduct high resolution microscopy over a wide array of surfaces without sample preparation.

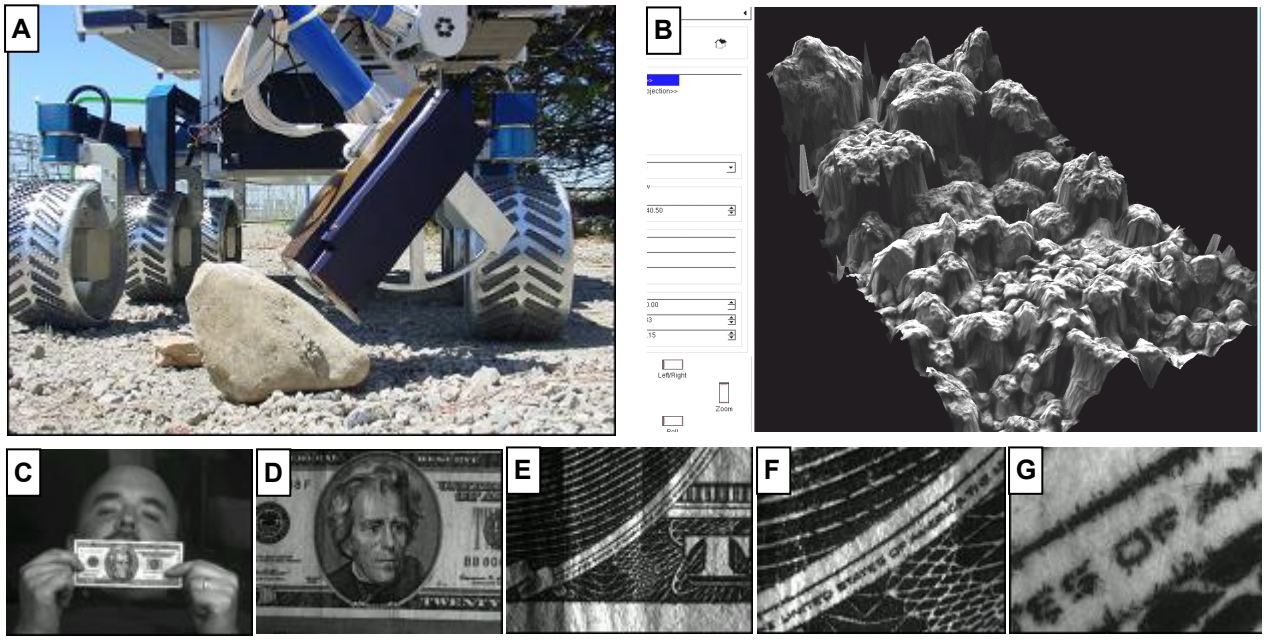

Fig. 1. MIDP CHAMP Instrument. A) MIDP CHAMP integrated on robot arm conducting microscopic investigation of rock. B) Example of focal-plane-merged image (courtesy of Matt Deans, NASA Ames). C) – F) CHAMP approach to a U.S.$20 [1,6].

In independent optical spectroscopic analysis and instrument development conducted under NASA's Astrobiology Science and Technology Instrument Development (ASTID) program, optical coupling[‡] onto microscopic features for conducting Raman[§] and micro-LIBS[**] laser spectroscopies of unimproved geologic surfaces was identified [6]. For the case of tightly-focused laser ablation techniques (e.g. micro-LIBS, time-of-flight mass spectrometry), laser fluence can readily vary by orders of magnitude over relatively short working distances. This variation in flux causes a corresponding large variation in gas/plasma temperature which typically degrades the quality of an instrument measurement utilizing ablation. In the case of micro-LIBS, the large variation in plasma temperature causes a corresponding larger variation in micro-LIBS emission signal complicating the accurate interpretation of relative elemental abundances [6, 7]. For Raman spectroscopy, the coupling is less sensitive, but still important for ensuring that the precious few laser photons that have been frequency shifted and contain chemical signature information are not lost, but rather efficiently collected into the optical system and ultimately into a spectrometer for spectral analysis.

Raman spectroscopy coupled with imaging is commonly limited to confocal imaging systems due to the issue of lens fluorescence in optical elements that can significantly degrade the measurement signal-to-noise. Given the larger number of optical elements, the feasibility of conducting Raman spectroscopy with a CHAMP imaging system was a concern. This concern was initially addressed by: 1) demonstrating low Raman fluorescence background measurements

---

[‡] Optical coupling as defined here is the focusing of laser light onto particular features within a field-of-view (most commonly microscopic) where the surface roughness varies by greater than the beam's depth-of-field.

[§] Raman spectroscopy utilizes the inelastic scatter of laser photons interacting with the rotational and vibrational modes in laser-illuminated molecules in order to identify the unique spectroscopic fingerprints of molecules contained within the laser spot.

[**] Micro-LIBS is a laser spectroscopic technique that allows one to estimate relative elemental abundance of a laser-illuminated spot by laser-ablating the spot with sufficient energy to generate a high temperature micro-plasma from the ablated solid, and subsequently observing the elemental emissions lines in the plasma as the plasma rapidly cools (<10 μs decay time typical).

after integrating the Mars Microbeam Raman Spectrometer with the MIDP CHAMP and 2) modeling of the Raman scatter inside CHAMP-SLS lens elements to demonstrate the strong suppression of lens fluorescence in the CHAMP-SLS system by passive lensing of the fluorescence photons out of a 6 dimensional Raman acceptance space[††] [8,9].

Micro-LIBS measurements generated the potential concern of lens contamination due to generation of plasma plumes in close proximity to optical elements. Initial contamination investigations using desiccated geologic samples as would be expected to be encountered in very low pressure (~5 torr), space environments were conducted with many 1000's of micro-LIBS pulses in the F/#4 beam configuration and working distances associated with the MIDP CHAMP instrument deployed at peak magnification (the ablation spot diameters are <10 micron typical). The conclusions from this work were that although high temperature gases and solid micro-debris was generated in close proximity to a CHAMP-like window, the expanding plasma plume rapidly cools creating a condensate that does not damage the window. In fact, 10,000+ repeated pulses generated only a light dust-like coating that was still transparent and easily cleared-off by very lightly wiping or blowing with compressed air [10]. In the absence of a window cleaning mechanism, this dust would effectively reduce the window transmission over long extended periods of micro-LIBS observational times. Ongoing work is investigating similar micro-LIBS contamination conditions using volatile-rich samples.

Based on this spectroscopy work, Raman spectroscopy and micro-LIBS appeared feasible to integrate with a CHAMP field imaging system. Under NASA's In-Situ Resource Utilization (ISRU) Program, the funding opportunity to design, build, and test a version of CHAMP-SLS imaging optical elements for purposes of lunar regolith characterization was provided. The research and development of the CHAMP-SLS optical elements is described in detail below.

2. METHODOLOGY

2.1 Optical Design Requirements/Goals

The optical spectroscopic version of CHAMP (designated CHAMP-SLS) had to incorporate additional derived optical requirements compared to the original MIDP CHAMP prior to initiating the extended design and optimization process which was iterated over 1.5 years similar to the design process utilized for the MIDP CHAMP. These requirements and development goals are summarized below.

2.1.1 Increased Magnification/Resolution Goals

The original MIDP CHAMP achieved ~3 to 3.5 micron/pixel imaging resolution at a peak magnification of 4.4x [1]. In order to allow the instrument to ultimately be used to conduct high resolution geomicrobiology and potentially astrobiology investigations, a goal to try and enhance the peak magnification of the CHAMP-SLS instrument was made. This requirement had to be iterative and also ultimately had to consider the actual manufacturing results and tolerances of the lenses with an "as-built" design.

2.1.2 Laser Scanning and Laser Beam Gaussian Mode Quality Requirement

The ability to selectively target a laser through the optical system anywhere within the field-of-view from microscopy to hand lens resolutions (~100 micron/pixel ultimate camera resolutions) and also be able to return spectroscopic information specifically registered to the particular laser-illuminated spot was levied on the design.

Because of the nature in which the geometric rays were incident on the original MIDP CHAMP focal plane, a laser, if focused on the focal plane, could not effectively be scanned across the two-dimensional object plane beyond <10% of the field-of-view of the MIDP CHAMP without significantly degrading the beam modal shape beyond the point where a micro-LIBS or Raman spectroscopic measurement could realistically be acquired through the CHAMP optical system [6]. As a result, a derived optical requirement for the geometric rays incident on the CHAMP-SLS focal plane were constrained to be normal to the focal plane within <3° for any laser wavelength that fell within the spectral bandpass identified below. The laser spot energy distribution on the object plane was required to fit a Gaussian profile with a root-mean-square error of <5% anywhere in the instrument field-of-view.

[††] For a given optical configuration, the corresponding 6 dimensional space of all laser-excited lens element volumes coupled with light propagation vectors which will allow a laser-excited fluorescence photon located in the volume to propagate into a Raman collection aperture.

2.1.3 Spectral Bandpass Requirement

Raman spectroscopy and micro-LIBS are corroborating measurements. Raman scattering typically covers wavelength shifts up to 4000 cm^{-1} (corresponds to 675.8nm for 532nm laser excitation). Micro-LIBS has a much broader required spectral bandpass from the near-UV to near-IR. Table 1 summarizes the spectral bands necessary to cover eighteen of the most common elements with a collective emission line strength range for these particular elements that covers a dynamic range in relative emission line strength of 100. These spectral bands were derived from investigating the emission line strengths of 8,250 of the strongest elemental emission lines in the NIST atomic emission database [11]. The CHAMP-SLS spectral passband was derived based on these spectroscopic measurement requirements. To improve spectrometer coupling over the wide passband, a goal of also being able to image in this wide passband was prescribed with the relaxed constraint that focus shifts would be permissible.

Table 1. micro-LIBS spectral band requirements that drove CHAMP-SLS optical design

Element	Spectrometer Range *(nm)*
H	486 - 656
C	711 - 940
N	744 - 939
O	715 - 926
Na	498 - 946
Mg	384 - 941
Al	394 - 877
Si	391 - 794
P	533 - 930
S	675 - 924
Cl	510 - 919
K	534 - 890
Ca	393 - 866
Ti	334 - 802
Cr	427 - 698
Mn	331 - 652
Fe	340 - 709
Ni	343 - 773
CHAMP-SLS	**331 - 946**

2.1.4 Optical System Fluorescence Goals

Because of the concern over possible fluorescence in optical elements, a design goal of achieving equivalent or lower fluorescence background than was observed with the MMRS/MIDP CHAMP integration described above was prescribed. To achieve this goal, in the design of the CHAMP-SLS lens cells, an experimental survey of low fluorescence glasses (532 nm excitation) that were optical material candidates based on index of refraction and Abbe number for the CHAMP-SLS optical design was undertaken. These glasses had to have lower relative fluorescence than the original CHAMP glass materials. Furthermore, a similar ray tracing analysis of the 6D Raman acceptance volumes (as described above) was investigated to determine the sensitivity of a particular optical design for suppressing fluorescence photons that would be collected in the Raman aperture.

2.1.5 Thermal Design Requirements

The CHAMP-SLS imaging system ultimately may need to operate in a non-terrestrial flight environment where the instrument could be exposed to large temperature extremes. A requirement was placed on the instrument to be able to accommodate very large temperature excursions (currently modeled down to –100°C where available optical material measurements have been made) by allowing only compensating adjustments in positioning of lens cell 1 relative to lens cell 2. In analyzing this requirement, the varying glass indices of refraction with temperature, the coefficients of thermal expansion (CTE) of the glass types, and CTE of candidate mounting materials (aluminum, titanium) when considering changes in lens spacings were taken into consideration.

2.1.6 Working Distance Goals

The original MIDP CHAMP instrument had a working distance at its 4.4x peak magnification of ~5-6mm [1]. To relax robotic arm placement constraints, the goal of increasing the working distance for a given magnification with similar MIDP CHAMP volumetric packaging constraints was prescribed.

2.1.7 Optical Range-finding Goals

Ultimately, for purposes of conducting field microscopy from a robotic arm, there is a need to precisely locate imaging targets in a 3D space for precision arm guidance, navigation, and control. Within any arbitrary field-of-view, any imaging target nested within this field-of-view should be state-observable (i.e. can be detected and precisely located). To provide this navigation requirement, characterizing the final correlation between focus distance (Lens Cell 1 to Lens Cell 2 distance) and range (i.e. working distance) was prescribed along with determining the optimized aperture function that would ensure the full field-of-view was state-observable particularly for short working distances.

2.1.8 Optical Element Count and Tolerancing Goal

Compared to the original MIDP CHAMP, a goal of reducing total optical element count and relaxing mounting tolerances was prescribed.

2.2 Optical System Iterative Design

With the optical constraints defined above, Zemax optical design/optimization software was used to selectively iterate through many hundred design configurations over the course of 1.5 years. Zemax optimization utilized multiple simultaneous working distance configurations of the CHAMP-SLS solved in parallel in order to force the Zemax design solver to provide a continuously variable magnification/working-distance design. Designs were selectively hand-picked and compared amongst one-another over the course of the design period to evaluate overall performance relative to the long list of requirements, constraints, and design goals described above. Design goals were modified and added based on the performance and characteristics of the best optical designs. Essentially, the overall CHAMP-SLS optimization involved both computer optimization based on optical constraints that could readily be fixed (e.g. hard requirements and parameters such as glass type constraints, instrument geometric constraints, magnification range, derived focal plane ray angle for scanning the entire field-of-view, and MTF performance for parallel working distance configurations) and a Darwinian-like selection process based on comparing performance amongst the candidate selectable designs (e.g. spectral bandpass performance, quality of imaging across the variable magnification, required optical and mechanical mounting tolerancing, temperature and wavelength focus shift compensation). The beam-split focal plane interface was iteratively derived after several architecture studies were conducted on how best to couple spectroscopy with imaging while simultaneously trying to return maximum spectroscopic emission signal to a corresponding conjugate focal plane pixel for any specific laser-illumination point located within the object plane field-of-view.

Glass selection was initially constrained based on published fluorescence data with a 550nm excitation source [12]. Expansion of this initial glass set and then final glass set refinement during the optical design process was provided by conducting relative fluorescence tests with a Kaiser Holoprobe system using 532nm laser excitation and a cooled CCD detector in a fixed focus configuration. The glass samples were pre-cleaned with dichlormethane and then all run (or normalized to) 5s integration times with 5 accumulations each. A blank (no sample) was run using an empty sample holder. Based on these relative fluorescence tests, glasses considered for the CHAMP-SLS design included: Schott F2, K5, NSF56, STIH23, Ohara S−BLS7, S−LAL8B, S−NBH8. Final fluorescence assessment at the design phase was conducted by assuming a volumetric lambertian emitter in each lens based on the excitation laser beam profile through the lens, calculating a geometric lens attenuation factor and relative lens fluorescence cross-section as previously described above, and assessing the resultant relative contribution of fluorescence from each lens in the system. Modifications were made to the optical system to reduce and balance relative fluorescence contribution across the system.

The final CHAMP-SLS design that was selected from this process was completely toleranced, sent out for bid, and finally fabricated by Optimax, Inc. Figure 2 illustrates Zemax ray traces for the CHAMP-SLS lens cells in three different imaging configurations. A fourth configuration is shown in which a concept Echelle spectrometer is coupled into one of the CHAMP-SLS focal planes for supporting future scanning laser spectroscopy. Fiber optic probehead coupling into one of the CHAMP-SLS focal planes is another alternative. CHAMP-SLS conservation of Etendue ensures that the original CHAMP-SLS distal end F/# during imaging is preserved throughout the optical system into the probehead as long as the spectroscopic probehead or optical system couples into one of the CHAMP-SLS focal planes with an F/#14 beam. Note this incident beam is, for all practical purposes, completely independent of CHAMP-SLS working distance/magnification as can be seen in the incident ray traces on the focal plane shown in Figure 2.

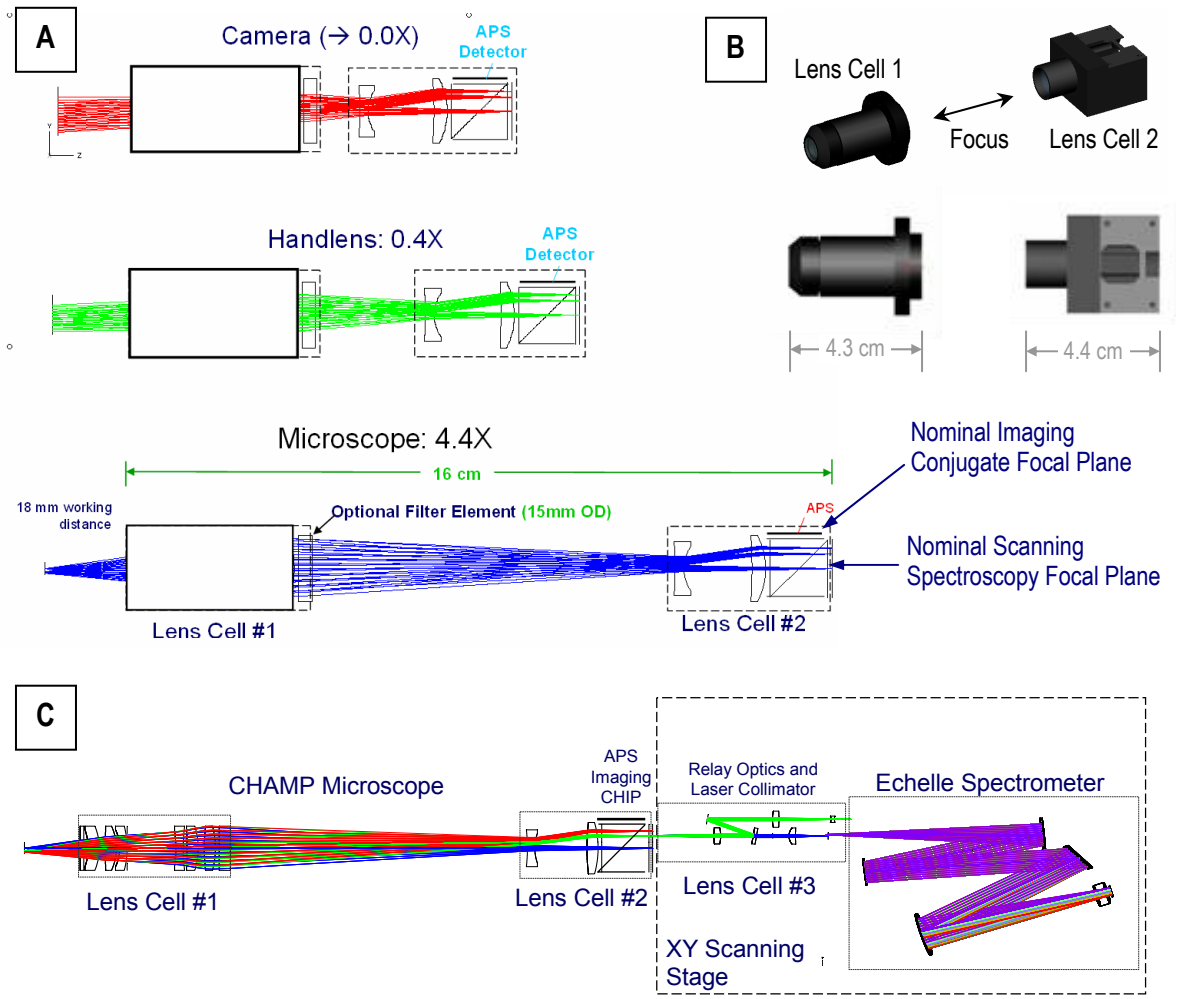

Fig. 2. CHAMP-SLS continuously variable imaging shown for A) three imaging configurations, 0.0X, 0.4X, and 4.4X. B) Concept integration of a scannable laser/Raman probehead free-space coupled to an Echelle spectrometer.

2.3 Optical System Fabrication and Initial Testing

2.3.1 Lens Fabrication, Quality Control Measurements, and As-built Design

Seven sets of CHAMP-SLS optical elements were produced based on the toleranced specifications provided from the final design generated as discussed in Section 1.2. The lenses included a MgF_2 anti-reflection coating. Upon receipt, the optics were organized and prioritized in terms of manufacturing quality based on 6 primary criteria: 1) Surface spherical aberrations, 2) Wedge, 3) Decenter, 4) Lens radii, 5) Lens thickness, and 6) Lens bevel edge quality. These criteria was established based on the ability to compensate for lens manufacturing variations from an idealized design based on final "as-built" design and lens mounting .

As part of the quality control process, each lens surface was interferometrically mapped and fit with a 36 coefficient Zernike polynomial. These polynomials were entered into Zemax in order to generate the final "as-built optics" optical system design. Due to simulation time-constraints for lens alignment optimization (calculated Zemax optimization simulation times would've exceeded 2 years on a 500 MHz P.C. workstation), a custom JPL optics model developed by co-author Gürsel was utilized to speed up the optical optimization process (2 day simulation time) in order to determine the final lens rotations and relative lens spacings. In this optimization process, axisymmetric asymmetries of the spherical aberrations for each of the individual optics were corrected collectively to minimize overall wavefront error.

Final optical element spacings deviated by up to 2mm relative to the original design based on this final "as-built" optical element realignment optimization process.

2.3.2 Lens Cell Design and Lens Mounting

The CHAMP-SLS toleranced lens cell designs, lens cell fabrication, optics mounting and laser alignment were subcontracted out to Optoalignment, Inc, a company who specializes in precision optical alignment and mounting including precision mounting configurations that have flown and survived launch vehicle environments.

2.3.3 Optical System Wavefront Testing

Upon receipt, the wavefront through the CHAMP-SLS lens cells were interferometrically measured with a ZYGO GPI-XP to have an RMS wavefront error across the entire clear aperture less than $\lambda/10$ for Lens Cell 1 and less than $\lambda/5$ for Lens Cell 2.

3. OPTICAL PERFORMANCE RESULTS

The following subsections summarize CHAMP-SLS key optical performance characteristics ultimately for conducting multi-scale imaging, field microscopy, and laser optical spectroscopy from a robot arm.

3.1 Spectral Transmission

Figure 2 illustrates the CHAMP-SLS spectral transmission at short wavelength as designed based on computing the glass extinction coefficients through each optical element derived from the optical element's glass absorption vs. wavelength and maximum optical element thickness. This optical design is not effectively transmission-limited in the near-IR. In the near-UV wavelengths for micro-LIBS investigations, the lower transmittance at 330nm (see Table 1 for transmission requirements) is easily offset by the much higher typical elemental emission line strengths justifying this design ability to meet the spectral emission lines constraints summarized in Table 1. Over CHAMP-SLS very large spectral range, diffraction-limited imaging (based on Zemax analysis) is effectively achieved through slight focus shifts between Lens Cell 1 and Lens Cell 2 (see Figure 4).

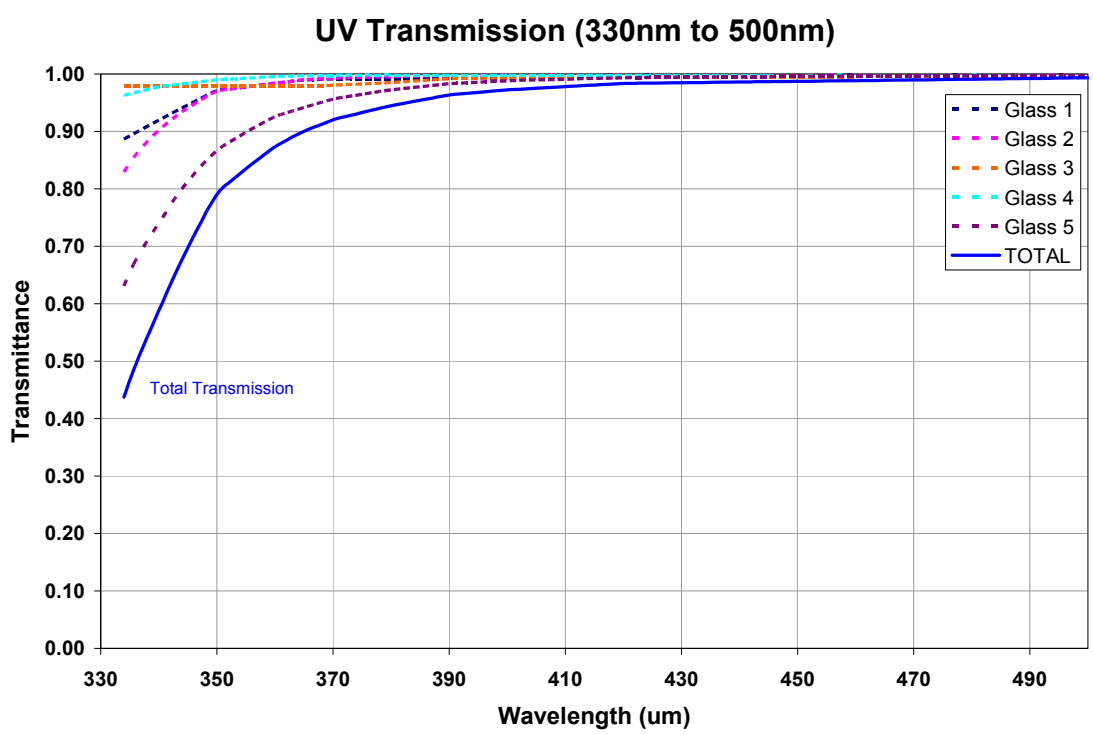

Fig. 3. CHAMP-SLS spectral bandpass in the vicinity of the near-UV cutoff. Calculated from lens thickness and individual glass-type extinction coefficients.

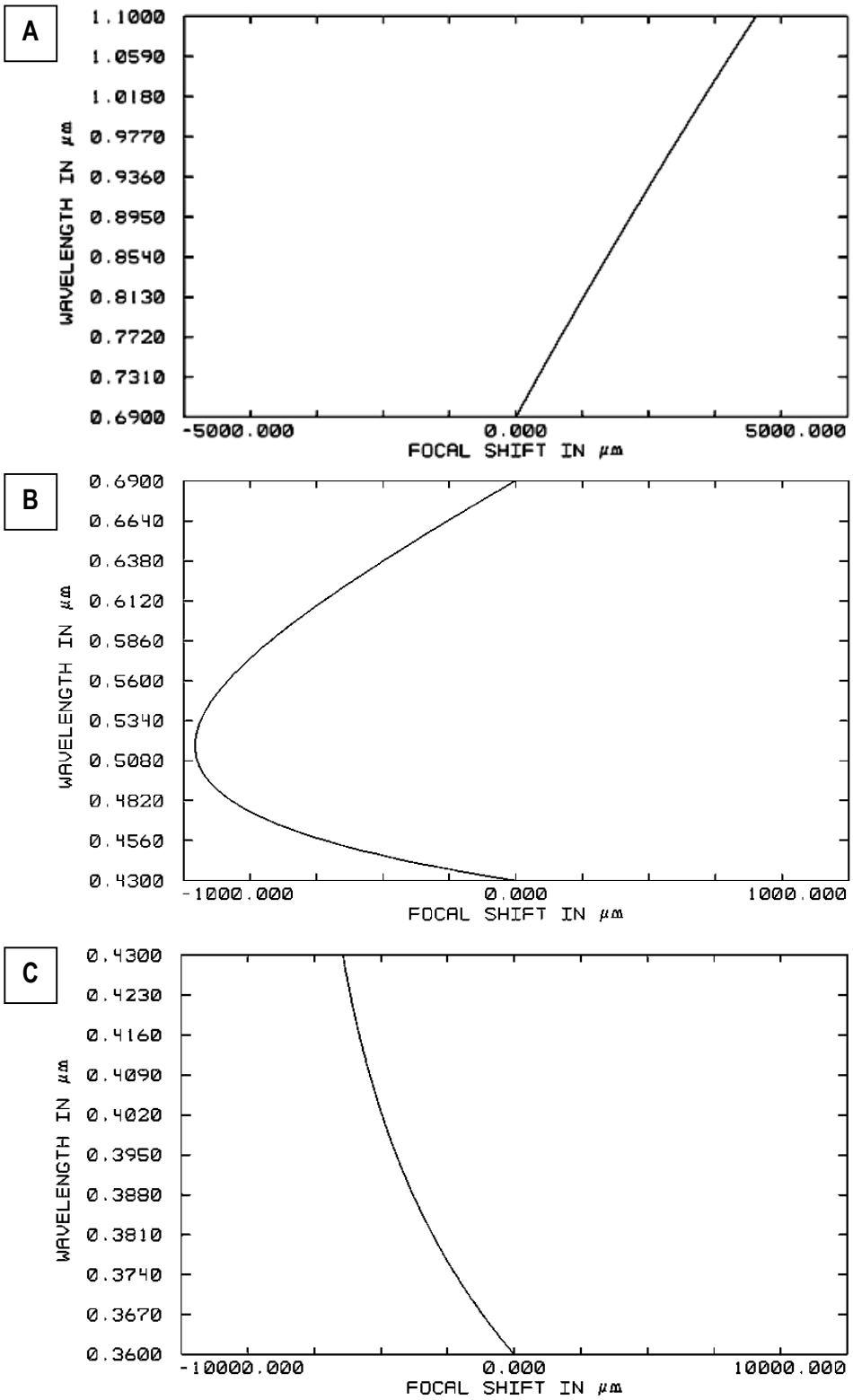

Fig. 4. Compensating focus adjustments over CHAMP-SLS' spectral range as a function of wavelength for M=4.4X. Note that in the visible spectrum from 0.430 microns to 0.690 microns, the shift in the image plane position is well within the diffraction-limited depth of focus across the spectrum in the paraxial limit. (Zemax model of "As-built" design).

3.2 Imaging Resolution vs. Magnification

The CHAMP-SLS imaging performance has been characterized under white light illumination in the visible range for a subset of arbitrary working distances and associated magnifications (M= 0.0189X, 0.1035X, 4.575X, 9.723X, 19.45X, 31.43X) sampled across CHAMP-SLS extensive imaging volume (see following subsections). To characterize imaging resolution across the field-of-view for these sampled working distances, two basic experimental methods have been employed: 1) Calculating the Sinusoidal spatial Frequency Response (SFR) by utilizing high contrast lines and a pixilated image at multiple sampled field points across the image (Star and Grid patterns), and 2) Imaging SFR targets. Imaging resolution in a complete imaging system configuration is ultimately dependent on many parameters including the optical system field modulation transfer function, pixel sampling frequency in the focal plane, pixel bit depth, pixel responsivity, applied light levels, and more advanced focal plane techniques that can be applied to achieve sub-pixel resolutions. We have, therefore, provided CHAMP-SLS object plane imaging resolution performance across the field-of-view based on the SFR for a cutoff contrast value of 0.3 and assuming Nyquist sampling in the focal plane (see Figure 5 for comparison in resolution as a function of contrast under peak saturation light levels). Depending on particular imaging applications, higher or lower cutoff SFR values may be used to estimate lower/higher values of imaging resolution respectively. To characterize the optical performance of the CHAMP-SLS lens cells, a Photonfocus 1024^2, 12bit CMOS camera was integrated into Lens Cell 2 and aligned to the conjugate focal plane (see Figure 6). Optimal lens cell boresight alignment was achieved by utilizing a ZYGO GPI-XP interferometer aligned through the same primary focal plane that ultimately would be utilized for conducting optical spectroscopy (see Figure 2). A similar alignment process is utilized for flight instruments prior to final bonding of optics and optics assemblies.

Based on this optical set-up, the following subsections illustrate imaging resolution measurements in the object plane as a function of magnification and associated working distance.

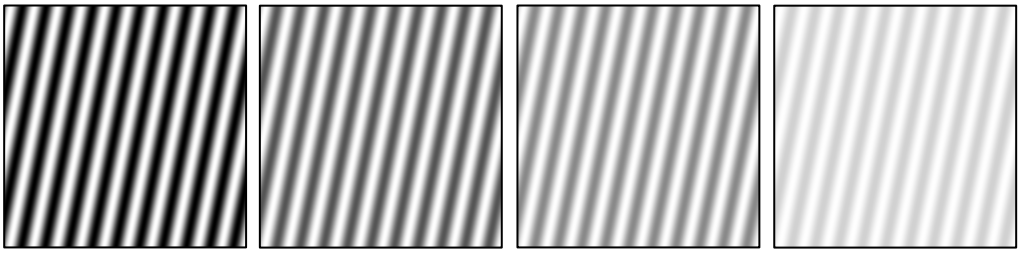

Fig. 5. Comparison of contrast for discernability. Contrast SFR values of [1.0, 0.5, 0.3, 0.1] (left to right) at peak intensity.

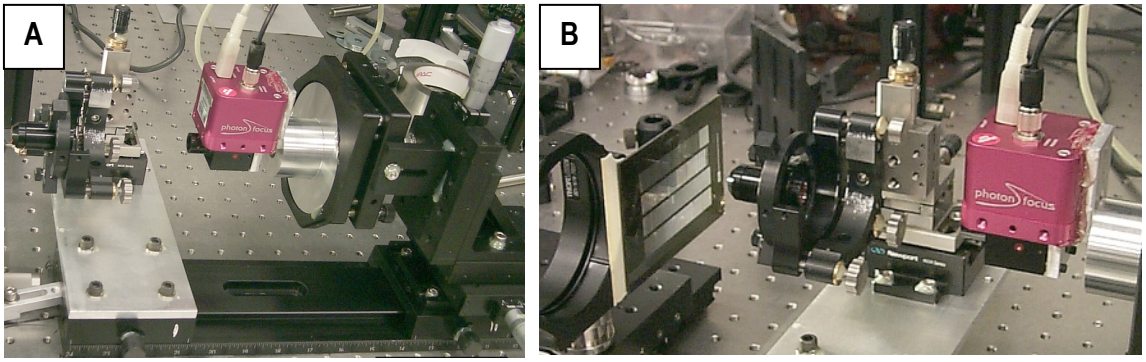

Fig. 6. CHAMP-SLS benchtop optical testing. A) Basic set-up with Photonfocus camera and translations stages for alignment and lens cell axial focus adjustments. B) Configuration for M=4.575X imaging resolution testing. In this case, a transmission sinusoidal MTF target is being imaged to verify SFR's derived from the star pattern targets as shown in proceeding figures. (Note benchtop hole spacing is 1" (2.54cm)).

3.2.1 Infinity Imaging: M = 0.01895X

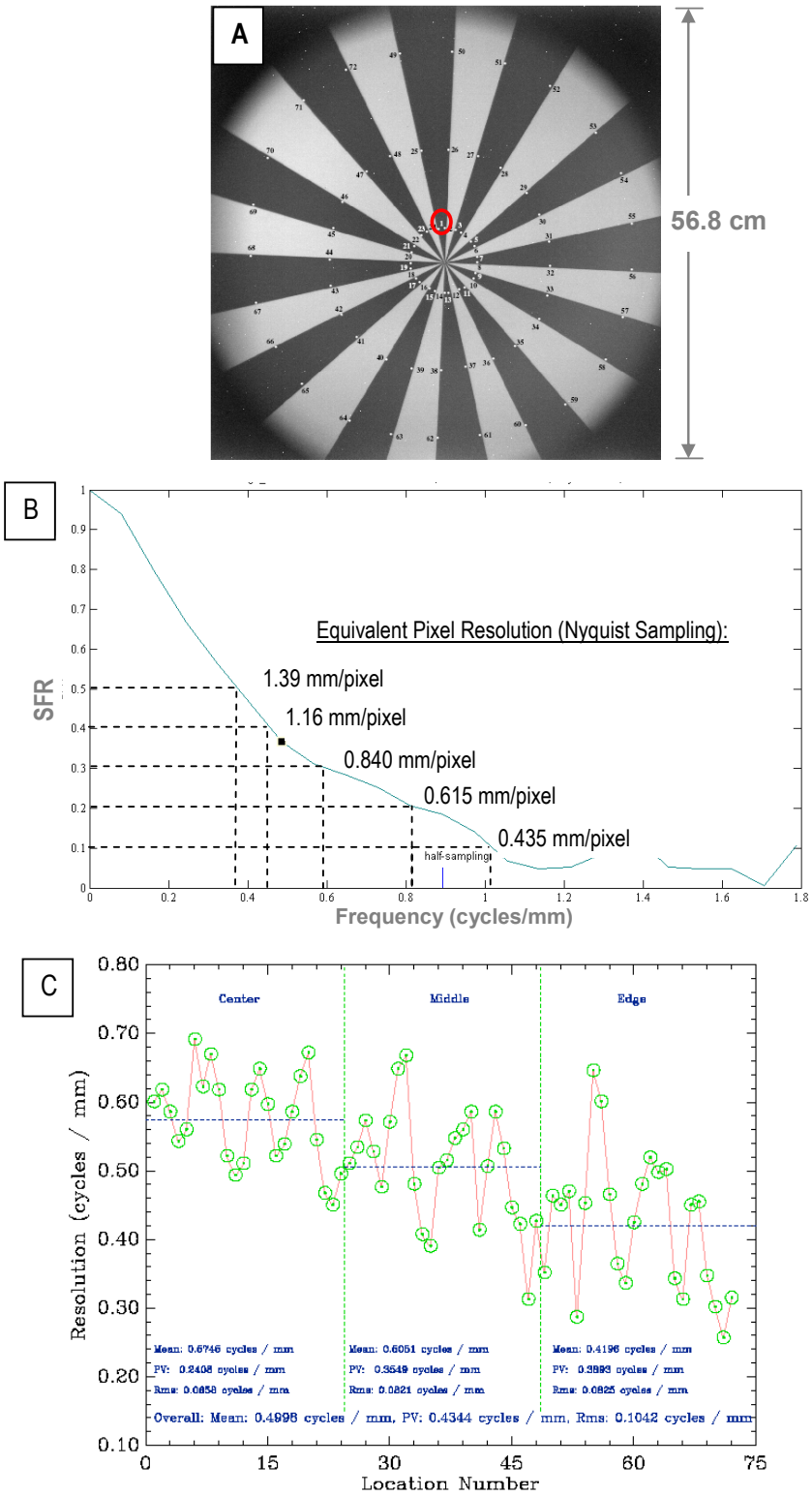

Fig. 7. Imaging resolution for CHAMP-SLS at magnification = 0.01895X. A) Image and spatial sampling for determining CHAMP-SLS' imaging resolution. B) Sinusoidal frequency response (SFR) at random exemplary field location 1 (red circle). C) Sampled imaging resolution statistics across field-of-view with cutoff SFR of 0.3.

3.2.2 Low Magnification Hand lens scale Imaging: M = 0.1035X

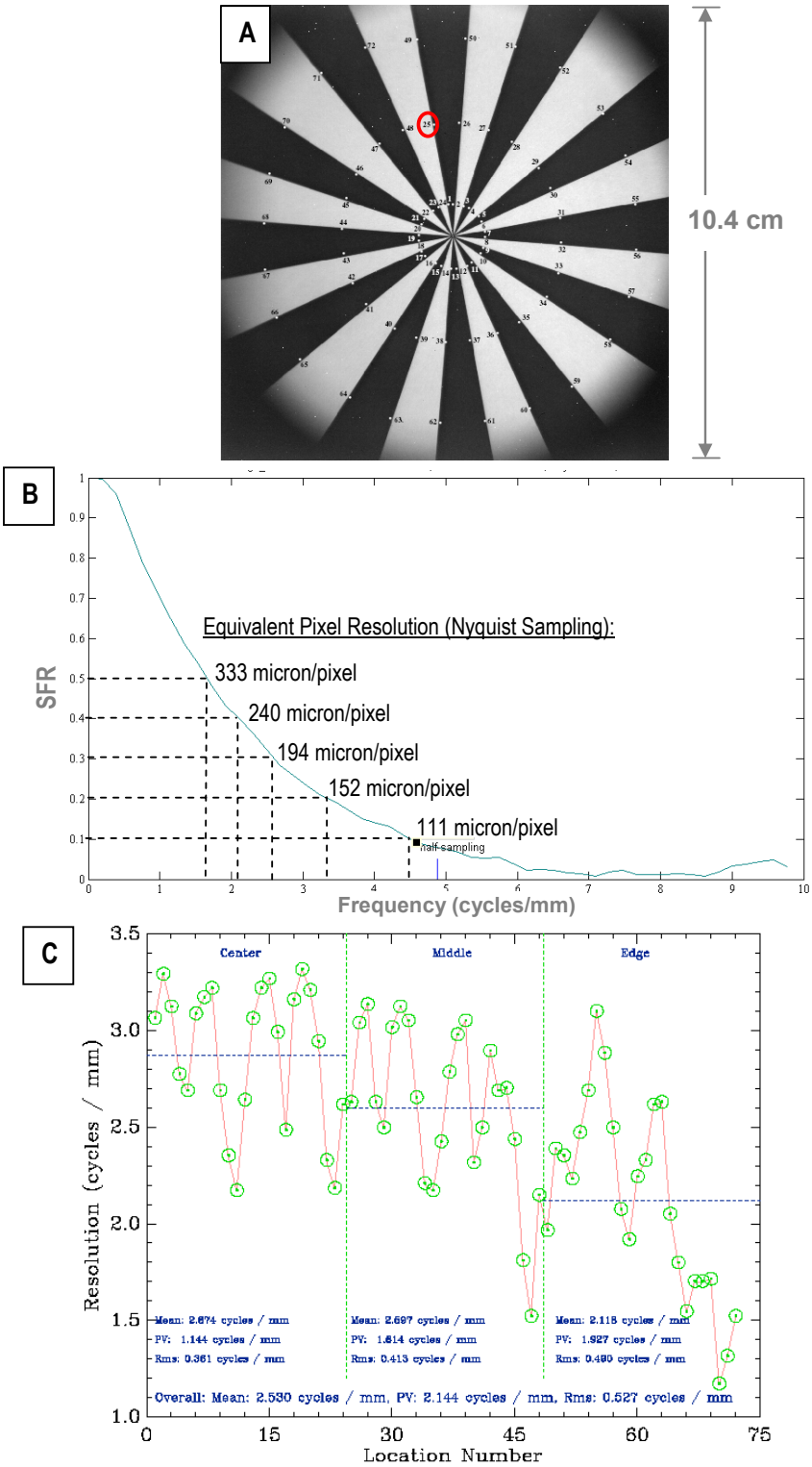

Fig. 8. Imaging resolution for CHAMP-SLS at magnification = 0.1035X. A) Image and spatial sampling for determining CHAMP-SLS' imaging resolution. B) Sinusoidal frequency response (SFR) at random exemplary field location 25 (red circle). C) Sampled imaging resolution statistics across field-of-view with cutoff SFR of 0.3.

3.2.3 Low Magnification Microscopy: M = 4.575X

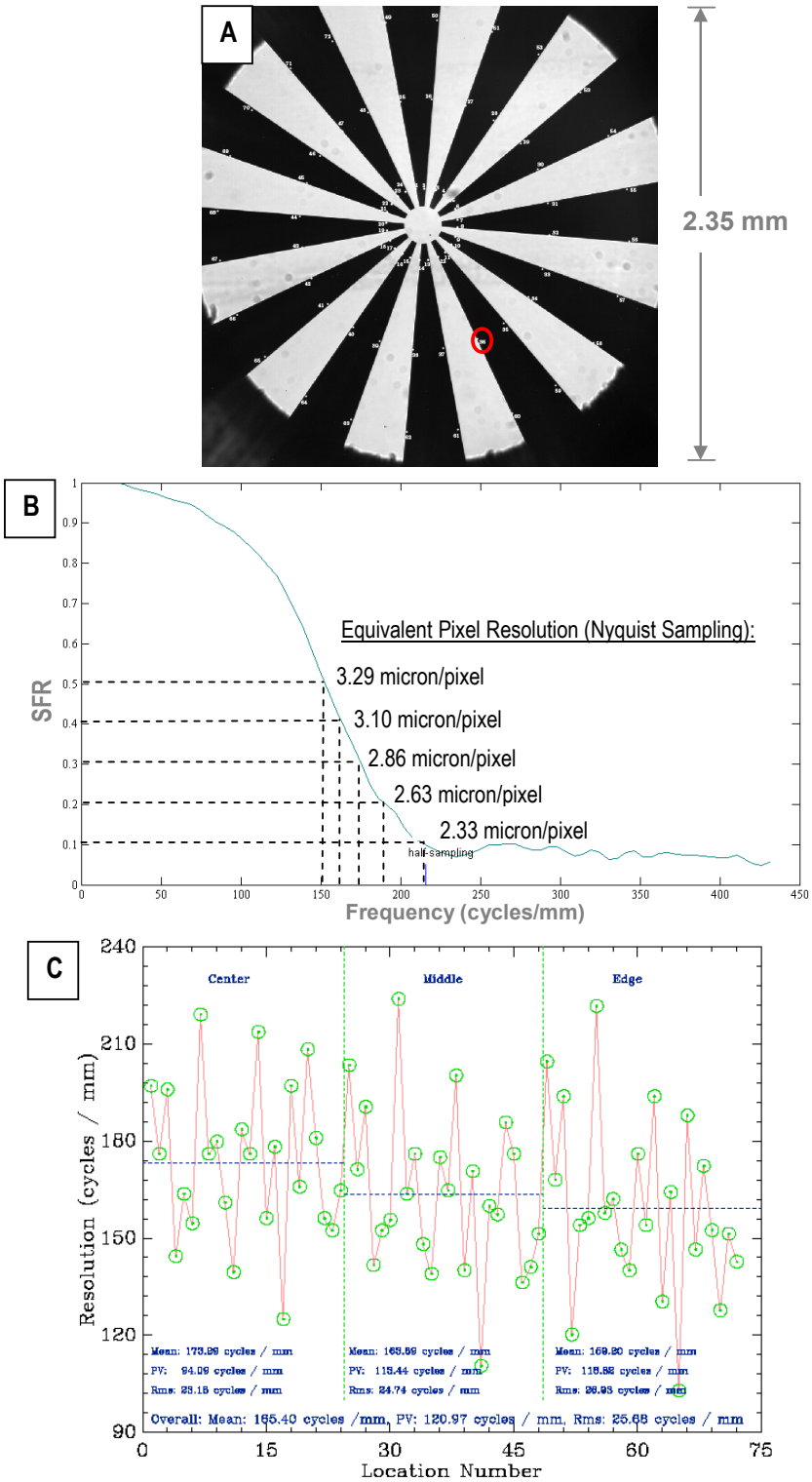

Fig. 9. Imaging resolution for CHAMP-SLS at magnification =4.575X. A) Image and spatial sampling for determining CHAMP-SLS' imaging resolution. B) Sinusoidal frequency response (SFR) at random exemplary field location 36 (red circle). C) Sampled imaging resolution statistics across field-of-view with cutoff SFR of 0.3.

3.2.4 Medium Low Magnification Microscopy: M = 9.723X

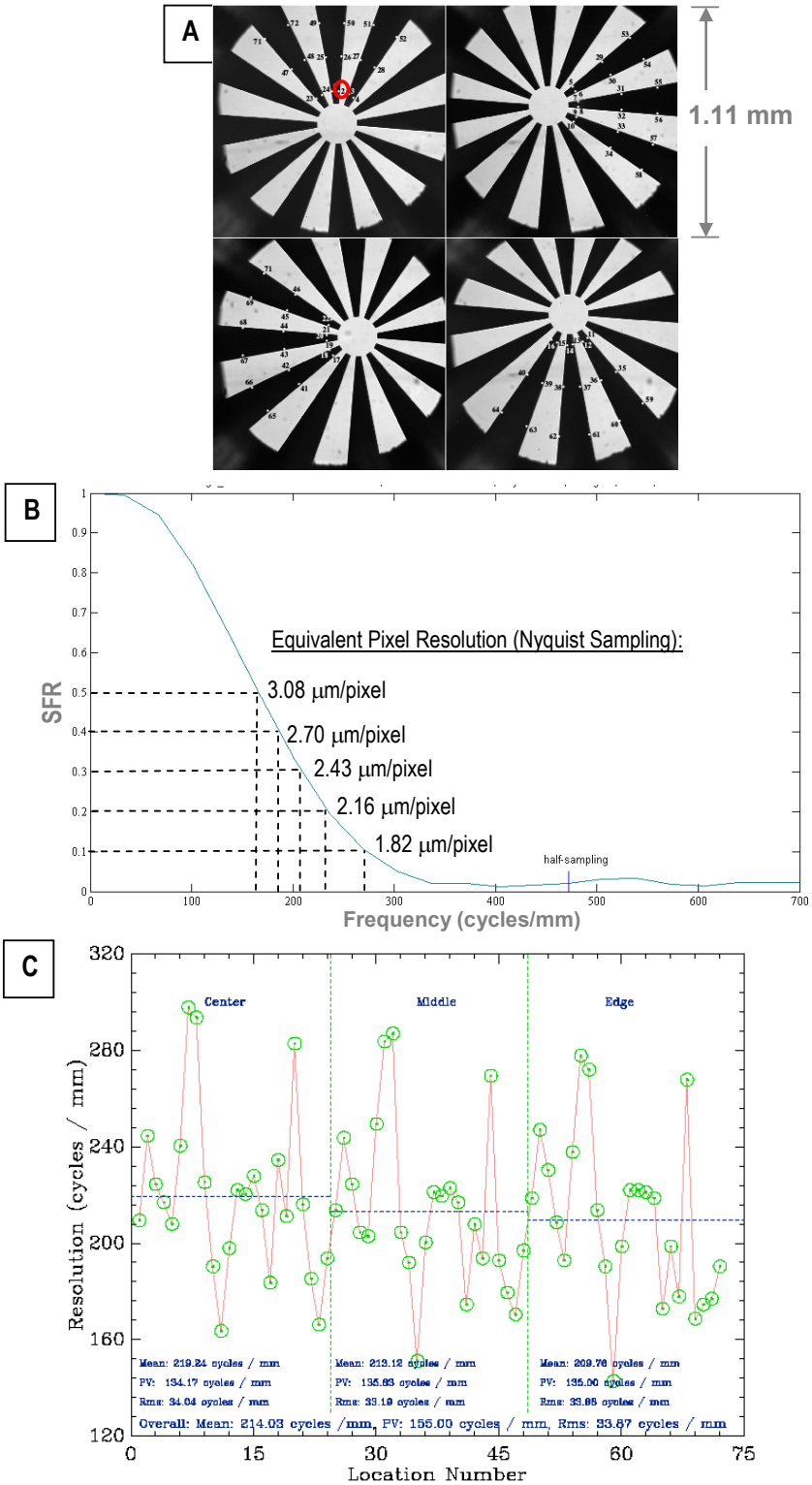

Fig. 10. Imaging resolution for CHAMP-SLS at magnification = 9.723X. A) Image and spatial sampling for determining CHAMP-SLS' imaging resolution. B) Sinusoidal frequency response (SFR) at random exemplary field location 2 (red circle). C) Sampled imaging resolution statistics across field-of-view with cutoff SFR of 0.3.

3.2.5 Medium Magnification Microscopy: M = 19.45X

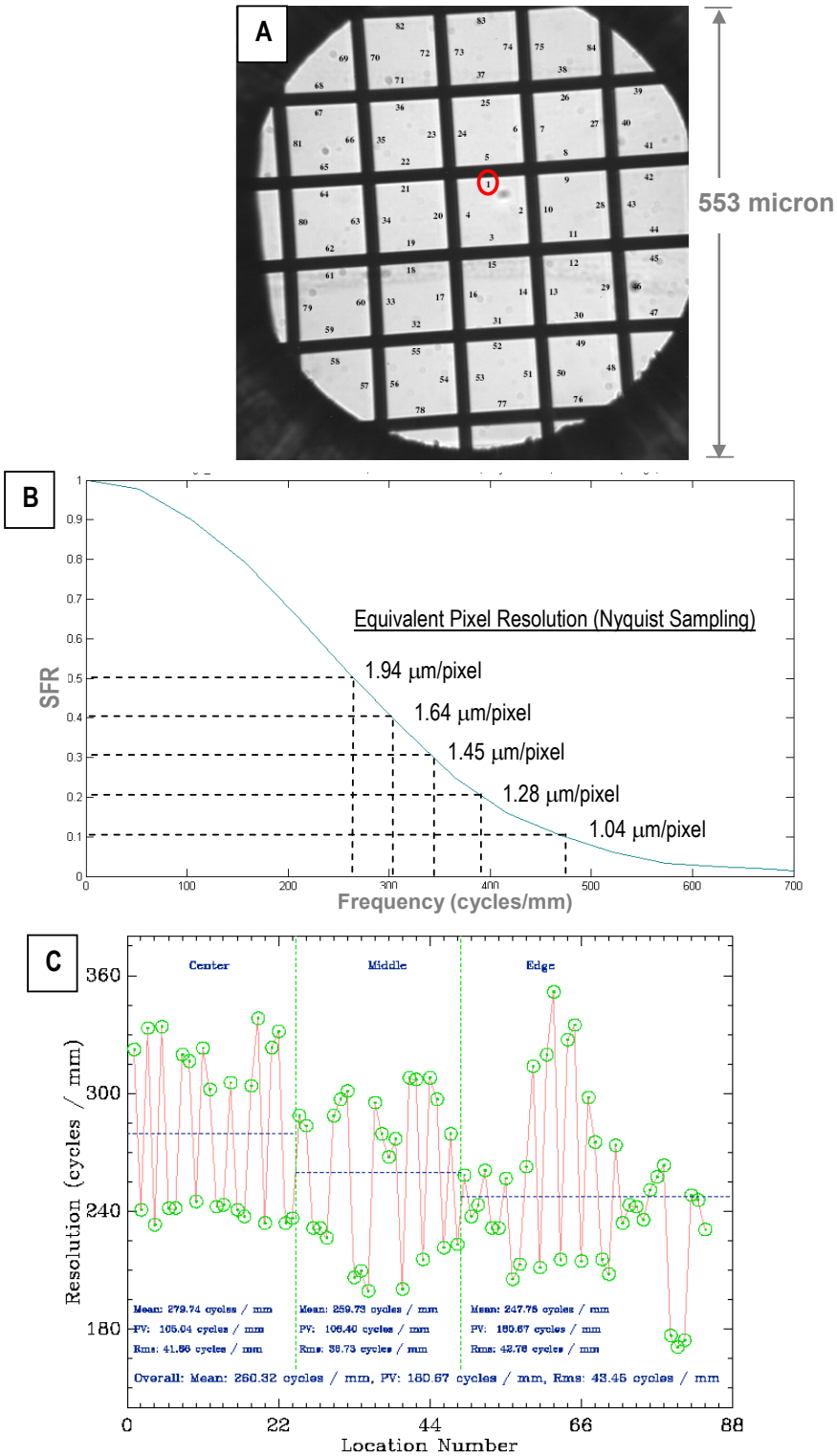

Fig. 11. Imaging resolution for CHAMP-SLS at magnification = 19.45X. A) Image and spatial sampling for determining CHAMP-SLS' imaging resolution. B) Sinusoidal frequency response (SFR) at random exemplary field location 1 (red circle). C) Sampled imaging resolution statistics across field-of-view with cutoff SFR of 0.3.

3.2.6 High Magnification Microscopy: M = 31.43X

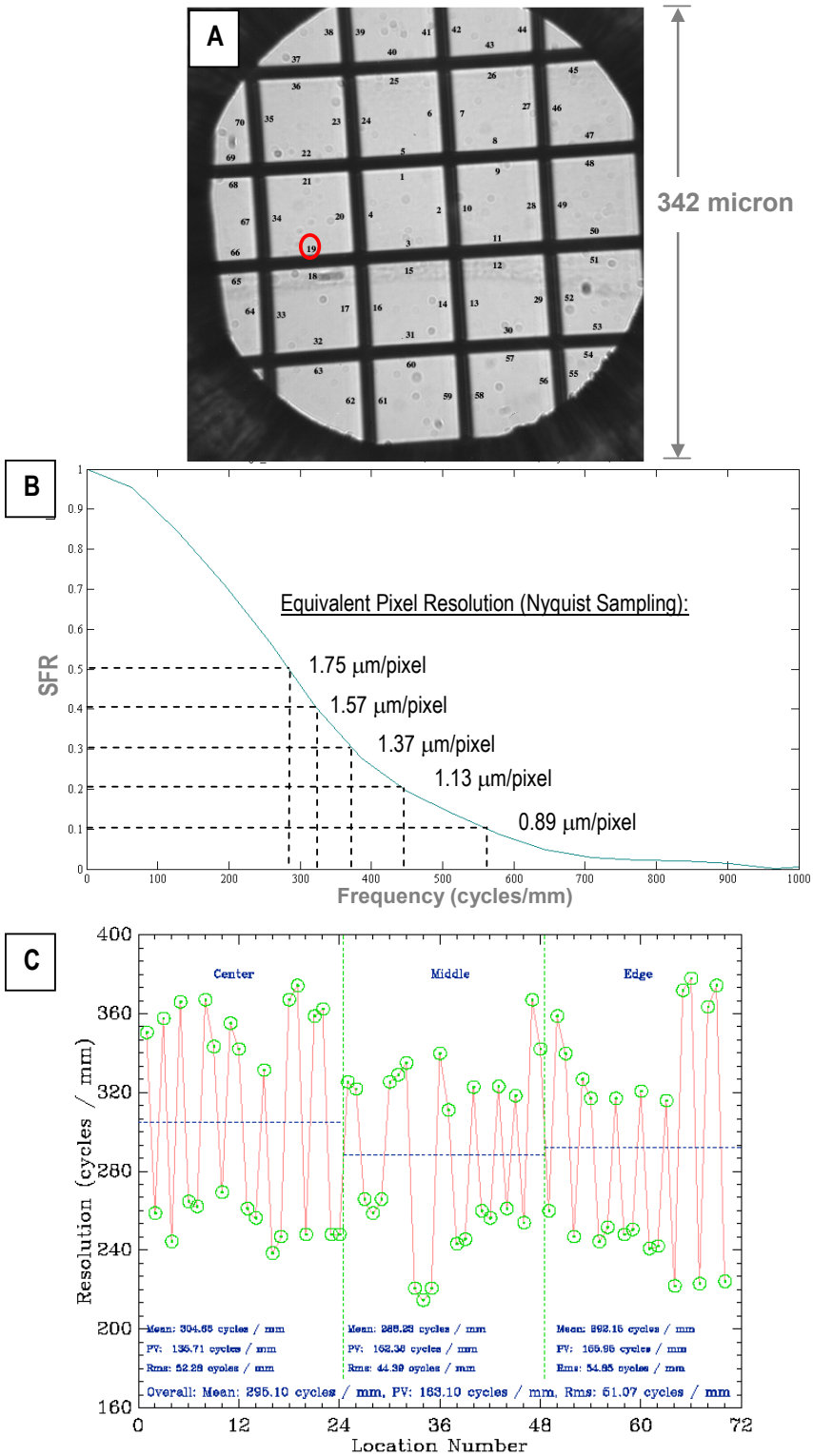

Fig. 12. Imaging resolution for CHAMP-SLS at magnification = 31.43X. A) Image and spatial sampling for determining CHAMP-SLS' imaging resolution. B) Sinusoidal frequency response (SFR) at random exemplary field location 19 (red circle). C) Sampled imaging resolution statistics across field-of-view with cutoff SFR of 0.3.

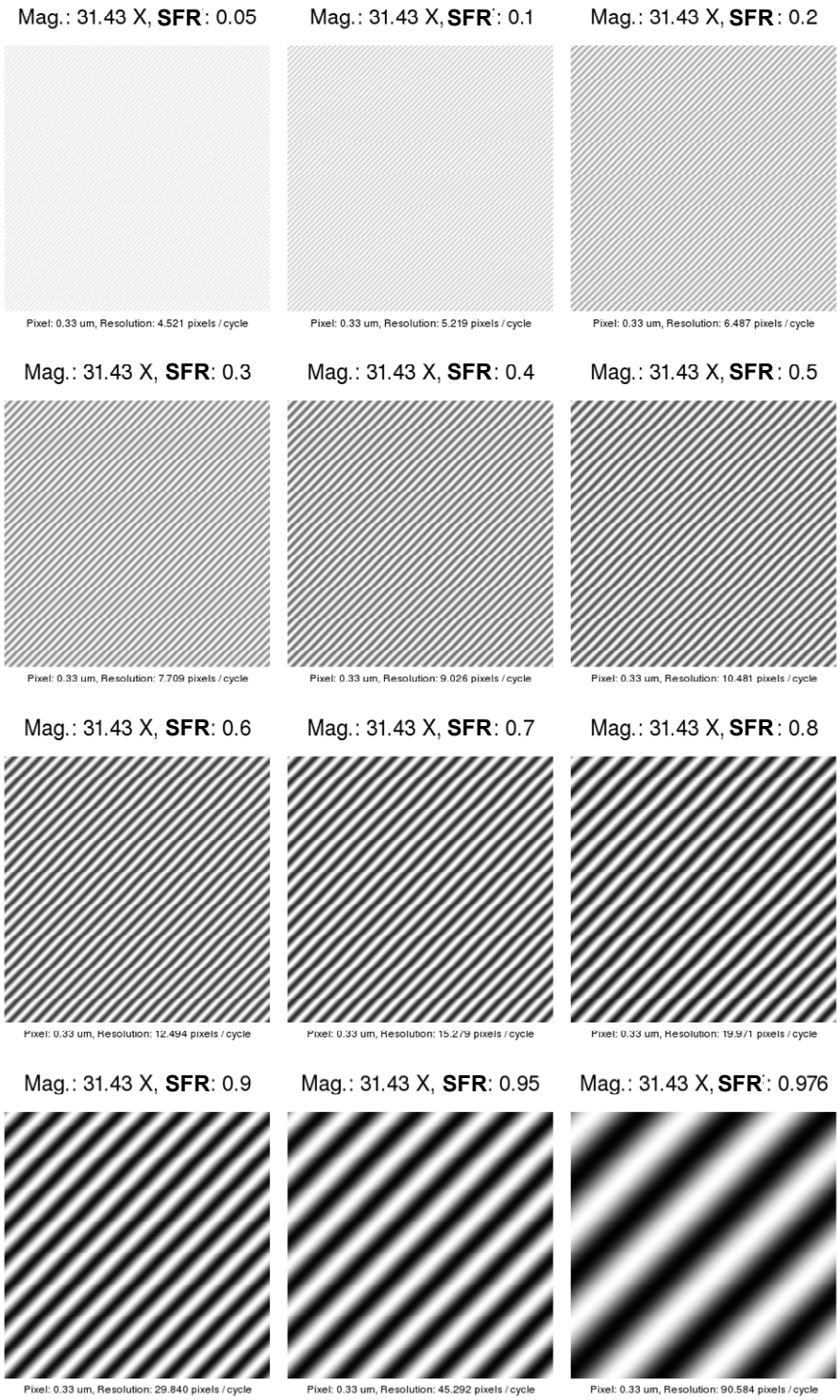

Fig. 13. Discernability for CHAMP-SLS at magnification = 31.43X. Plotted is a worst case 45° sinusoidal intensity pattern with varying relative intensity and sinusoidal spatial frequency (set to be the same along x and y axes) based on the Figure 12B SFR curve. The perceived frequency of the sine wave along this diagonal is actually higher by a factor of $\sqrt{2}$. If the sine wave were to be aligned along an x or y axis set to the same spatial frequency, the contrast would be slightly higher because of a lower effective spatial frequency.

3.2.7 Imaging Resolution vs. Working Distance/Lens Cell Position

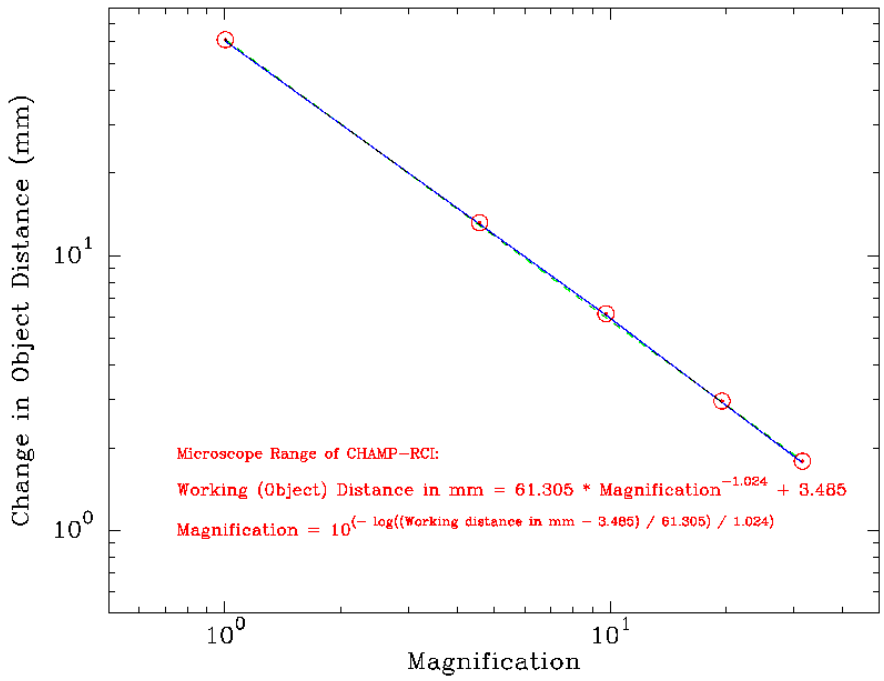

Fig. 14. Object distance vs. magnification illustrating power law relationship of CHAMP-SLS lens system behaving as chromatically-compensated thin lens with a magnification exponent very near -1.

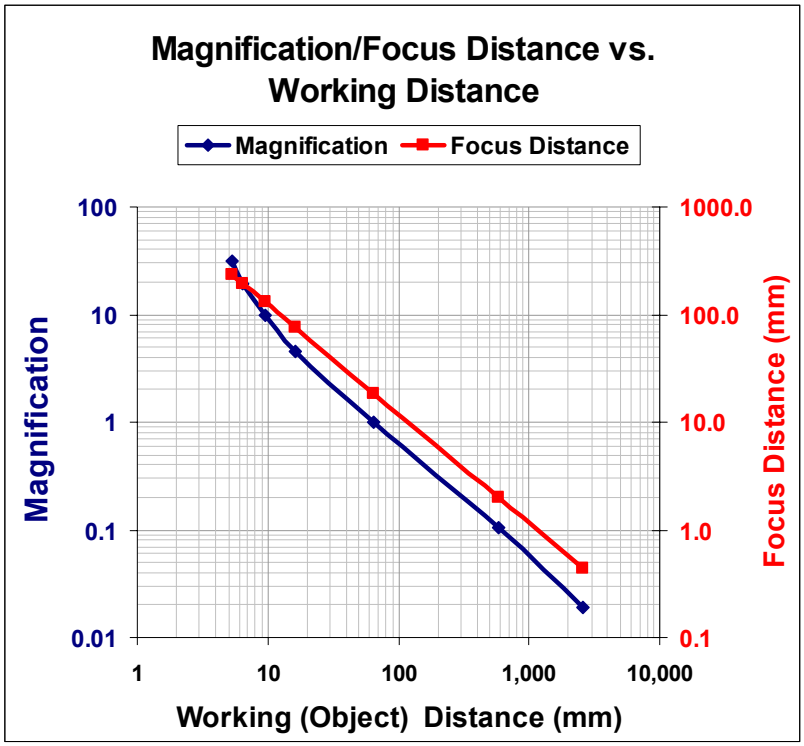

Fig. 15. Measured correlation between Working distance, Magnification and Focus Distance between Lens Cell 1 and 2

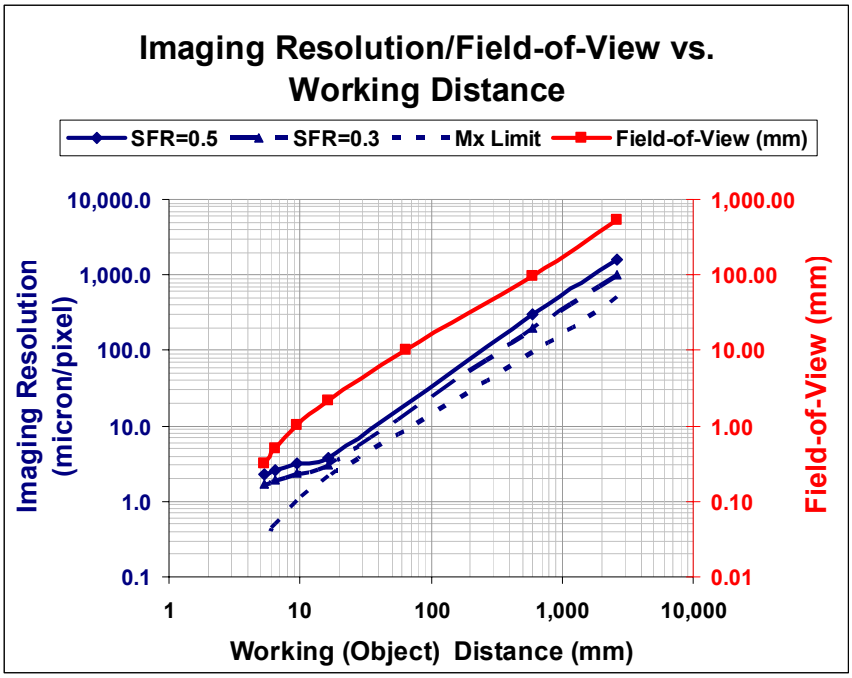

Fig. 16. Measured correlation between average field imaging resolution (cutoff SFR = 0.3, 0.5), Geometric magnification limit assuming 10 micron pixel, and Field-of-View for a 1cm detector

3.3 Range-finding Performance

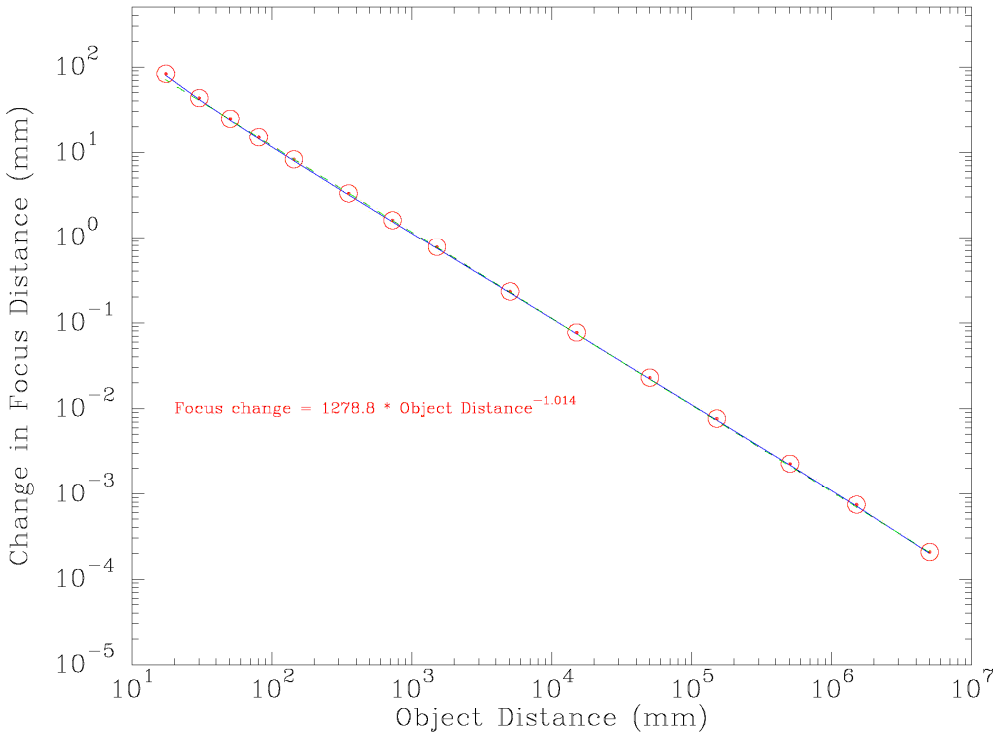

Fig. 17. CHAMP-SLS telescope range-finding performance (Focus distance vs. Object (working) distance) demonstrating lens system behaving as chromatically-compensated thin lens (object distance exponent near -1).

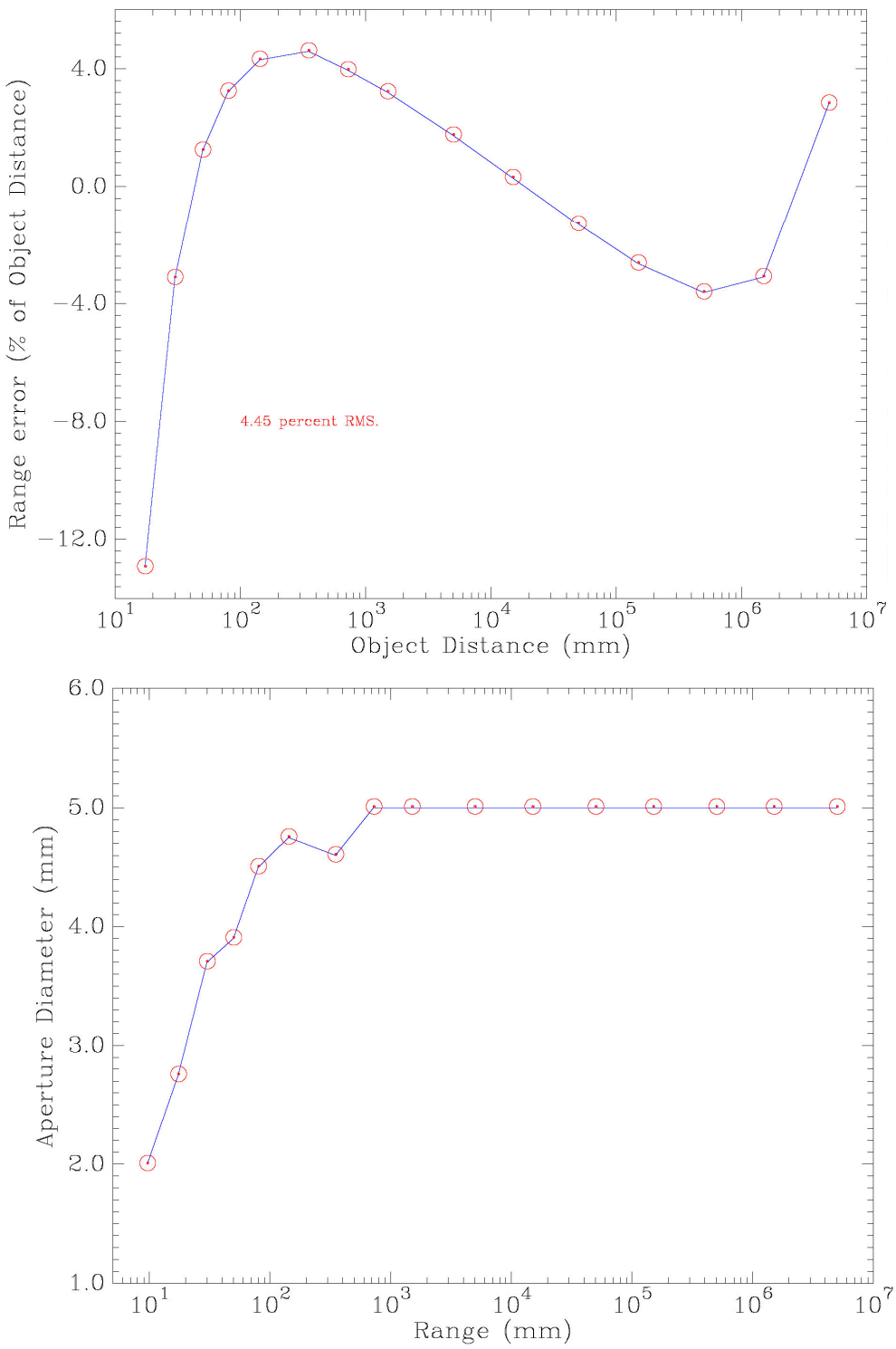

Fig. 18. Correlation between CHAMP-SLS range-finding error and actual range to target (*top*) when using the optimized aperture function (assuming an aperture for specific case of range-finding) as illustrated in (*bottom)* figure. The aperture makes entire field-of-view selectable for target range-finding.

3.4 Temperature Compensation

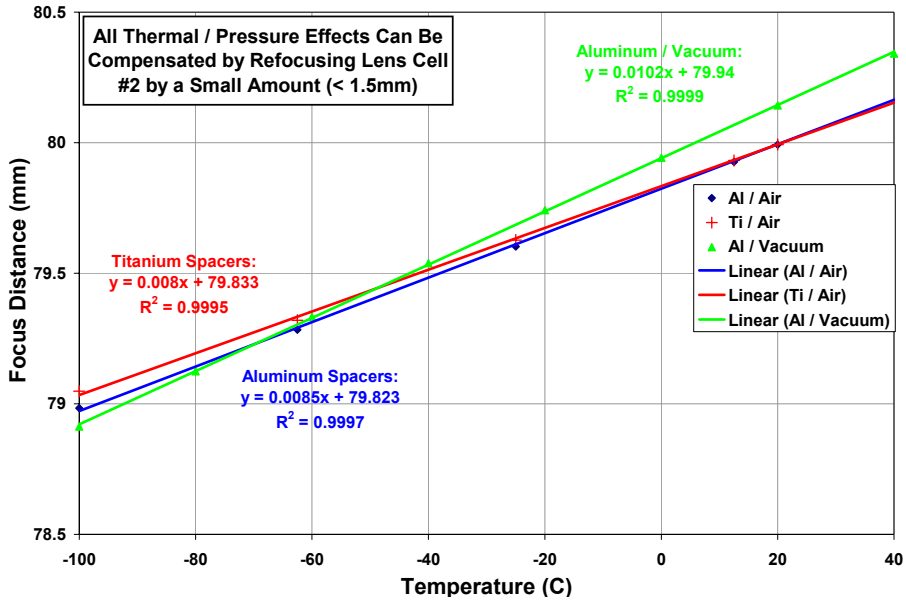

Fig. 19. CHAMP-SLS response to extreme temperatures through slight focus shifts to maintain MTF imaging performance at magnification of 4.4X.

3.5 Scannable Laser Beam Profiles

The entire CHAMP-SLS field-of-view is designed to be laser-scannable across the object plane by coupling an F/#14 beam into the image plane. The corresponding object plane laser spot size will be a scaled spot size corresponding to the working distance/magnification relationship identified in Figures 14,15 up to the point that the object plane beam's diffraction limit is reached. To test the actual laser beam profile as a function of field-of-view location, a 532nm laser weakly coupled into a single-mode fiber was used to produce a TEM00 mode Gaussian beam profile with an RMS <1.1% of Peak Intensity (Figure 20A). This beam was coupled into the numbered field point locations shown in Figure 20B. Figure 21 illustrates the measured variation in spot size as a function of field location for M=4.4X. This measurement was conducted by using two different axial distance beam profile measurements (5 and 20 cm's away from focal point) to infer the size of the beam waist at CHAMP-SLS corresponding focal point.

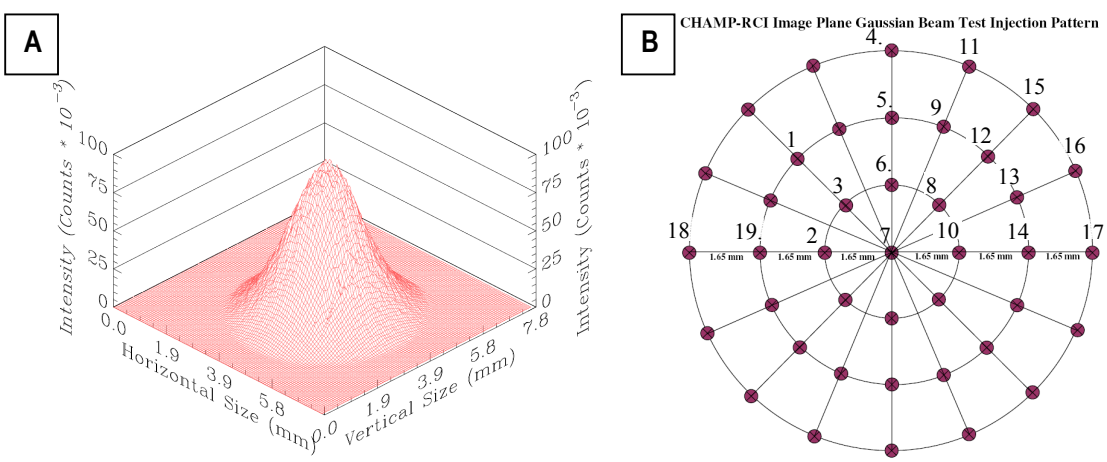

Fig. 20. Image plane injected 532nm laser beam characteristics and field-of-view sampling of laser profiles. A) Measured TEM00 laser beam profile used for beam profile testing, B) CHAMP-SLS image plane test points (numbered).

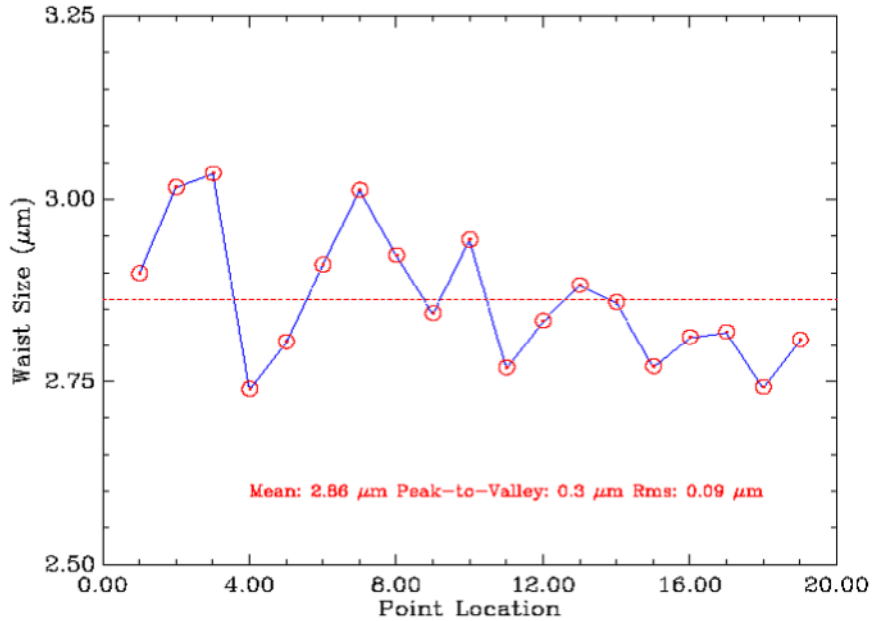

Fig. 21. Object plane variation in 532nm beam waist at CHAMP-SLS object plane focal point for M=4.4X as a function of field point location (defined in Figure 18B).

3. DISCUSSION

The previous sections describe the design, development, and optical testing of two relatively small lens cells that ultimately should provide the following capabilities for the CHAMP-SLS instrument: 1) a wide spectral-band (near-UV through near-IR) imaging system capable of spatially imaging from infinity continuously down to high resolution microscopy (~1 micron/pixel resolution at peak magnification); 2) precision optical range-finding capability for providing the ability to map surfaces in three-dimensional space as well as provide precision guidance feedback to robotic arms and/or actuators emplacing the instrument (particularly at high magnification where the imaging fields-of-view are extremely small); 3) ability to couple a laser and/or point spectrometer that can be scanned across the field-of-view of the instrument at any magnification with spot resolution at the pixel limit in an image; 4) accommodation of very high magnification imaging of unimproved/rough surfaces through small calibrated focus shifts; 5) diffraction-limited imaging performance over the wide spectral bands identified above through small calibrated focus shifts, and 6) accommodation of large temperature extremes through small calibrated focus shifts.

Utilizing the capabilities identified above, a laser spot can ultimately be precisely focused and scanned across any complex surface that falls within CHAMP-SLS extensive imaging volume even in rather extreme temperature environments. Collected scattered and/or reflected light from a laser-illuminated spot that falls within CHAMP-SLS' large spectral bandpass can ultimately used to infer chemical information from a particular laser-targeted spot. Alternatively, CHAMP-SLS can be coupled to other instrumentation to precisely target lasers for alternative spectroscopic techniques such as laser ablation mass-spectrometery.

All of the basic functions described above are provided by a single actuated axial degree of freedom between the lens cells. In the case of a scannable laser, an additional one or two degree-of-freedom scanning mechanism can be used to independently target a laser through the CHAMP-SLS optical system and across the field-of-view (e.g. using reflectance scatter from a low power laser pulse for relative targeting in the focal plane relative to an imaged target) without affecting the imaging functions previously described.

The data described in the previous section and subsections demonstrates the CHAMP-SLS' lens cells' ability to currently meet and exceed the original optical design requirements and goals originally set worth for the CHAMP-SLS instrument. Experimental measurements made, thus far, have been restricted to the visible imaging range. In future

work, similar experimental imaging resolution measurements will be made in near-UV and near-IR spectral bands. Furthermore, laser spectroscopic measurements will be conducted through the CHAMP-SLS optical system and compared to "gold" standard measurements utilizing state-of-the art laboratory probe-heads specifically for Raman spectroscopy, micro-LIBS, and Reflectance spectroscopy. More advanced focal plane analysis techniques coupled with relative motion will also be considered for augmenting the imaging resolution of the overall CHAMP-SLS system. This work will complete the precursor benchtop testing of the CHAMP-SLS Lens Cells prior to these Lens Cells being integrated into an instrument mechanical chassis and further integrated onto a robot arm similar to the MIDP CHAMP for purposes of robotic field-testing (see Figure 1). Figure 22 illustrates candid monochromatic images acquired during this initial phase of testing of the CHAMP-SLS instrument.

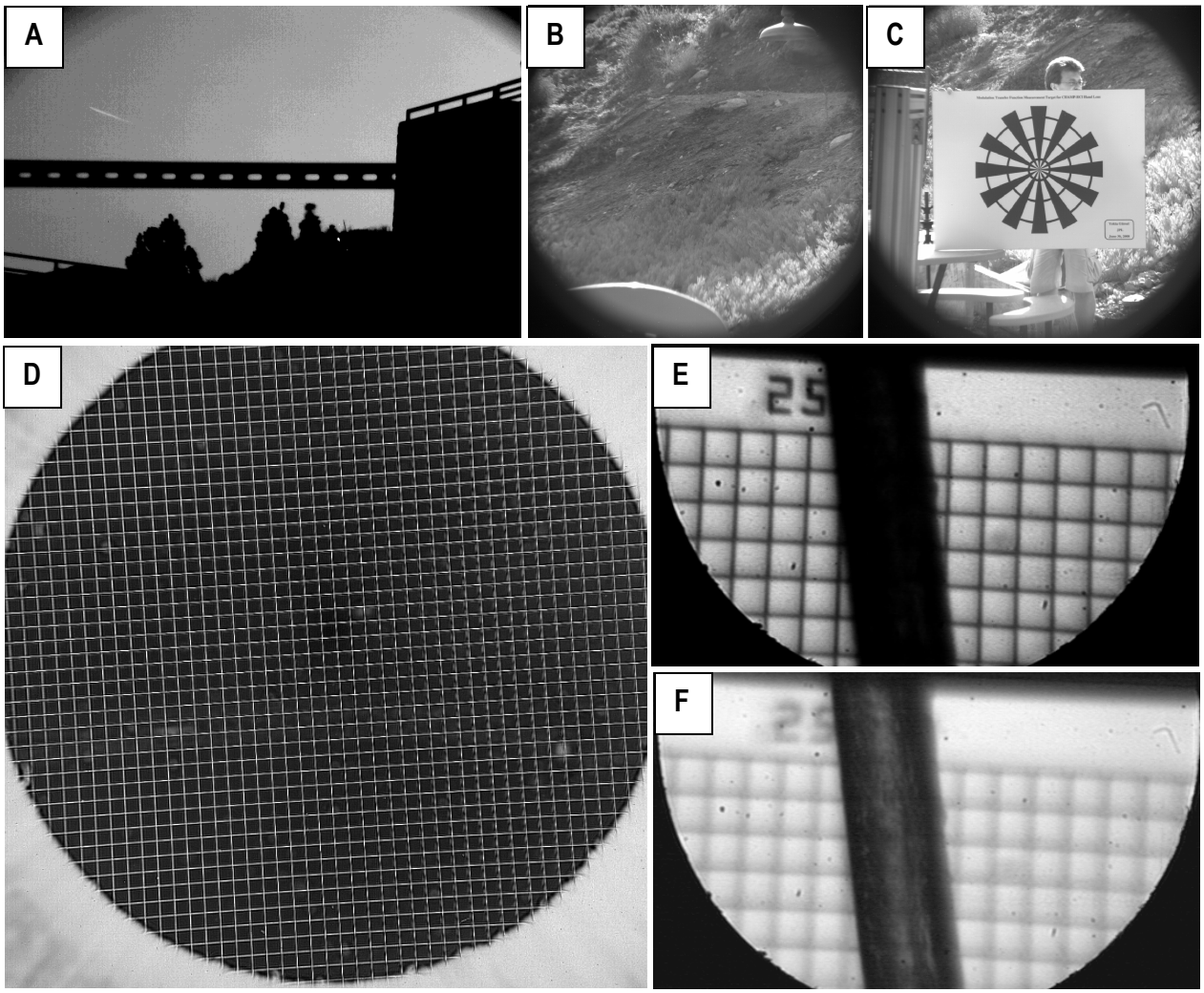

Fig. 22. Collage of monochromatic images acquired from CHAMP-SLS at progressively shorter working distance/higher magnification. A) 8-bit deep, CHAMP-SLS distant infinity image of airplane contrail near evening. B) 12-bit deep, far-field image of hillside. The edge of a plastic chair at the bottom of the image and the water shower head at the top of the image are located at a much shorter working distance (about 20 feet). C) 12-bit deep, macro-imaging of initial MTF target positioning at half the working distance of the hillside shown in B, at about 25 feet). D) Macro-lens image of 0.5 mm grid at M ≅ 1 X (11mm diameter field-of-view in image plane). E) Microscopic image of ~75 micron human hair emplaced on 25 micron grid target (target in focus). F) Microscopic image of ~75 micron human hair emplaced on 25 micron grid target (the hair in focus as can be seen by the imaged fine structure on the surface of the hair). Note z-stack depth-of-field compensation has not yet been implemented in the CHAMP-SLS instrument (see Figure 1B). (D), (E) and (F) are taken with the low resolution camera (640 x 480 pixels, as opposed to the 1024 x 1024 pixels of the 12-bit PhotonFocus camera used in all MTF characterization measurements).

4. CONCLUSIONS

This paper describes the design, development, and initial optical testing of an advanced imaging/spectroscopy instrument (CHAMP-SLS) that ultimately will be field-deployed on a robotic arm similar to its precursor, the MIDP CHAMP instrument. A list of instrument optical performance requirements have been derived from prior field microscopic investigations with the MIDP CHAMP instrument as well as laboratory optical spectroscopic measurements. The optical performance requirements and capabilities identified from these earlier studies are important for ultimately being able to conduct high spatial resolution spectroscopy investigations in an extreme field environment as would exist on another planetary surface or in space environments, in general. Based on optical measurements conducted to date, the optical performance of the designed and fabricated CHAMP-SLS lens cells meets and/or exceeds the original requirements and goals initially set forth. Future testing will extend the optical measurements into the near-UV and near-IR spectral bands and provide an opportunity to conduct coupled optical spectroscopic measurements.

For NASA applications for which it has been funded, the CHAMP-SLS instrument may eventually be deployed on a robotic arm or alternatively integrated with a space-suit with a visual heads-up display in order to relay visual and nested chemical information over a very wide range of imaging scales and spectral bands.

ACKNOWLEDGEMENT

The research described in this paper was carried out at the Jet Propulsion Laboratory, California Institute of Technology. This work expands on work previously conducted under the Mars Instrument Development Program (MIDP CHAMP) at the Laboratory of Atmospheric and Space Physics, continued on as the Raman CHAMP Instrument (RCI) funded as part of the RESOLVE project under the National Aeronautics and Space Administration's ISRU Program, and finally completed as CHAMP-SLS under JPL Director's Research and Development Funding (DRDF) Program .

DEDICATION

We'd like to dedicate this work to our former JPL colleague Cesar Sepulveda who left this world on June 22, 2008. His optical designs opened our eyes to Mars on Mars Pathfinder. As with all of his work conducted in the spirit of ultimately improving the lot for all, may his dedicated and hard work on CHAMP-SLS live on…

REFERENCES

[1] Boynton, J. , Mungas, G., Sepulveda, C., Fisher, T., Deans, M., Klein, D., Balzer, M., Beegle, L., Lee, P., Sobel, H., "Camera, Hand lens, And Microscope Probe", IEEE Aerospace Conference #1510 (2005).

[2] Herkenhoff, K.E., Squyres, S.W., Bell, J.F., Maki, J.N., Arenson, H.M., Bertelsen, P., Brown, D.I., Collins, S.A., Dingizian A., Elliot, S.T., Goetz, W., Hagerott, E.C., Hayes, A.g., Johnson, M.J., Kirk, R.L., McLennan, S., Morris, R.V., Scherr, L.M., Schwochert, M.A., Shiraishi, L.R., Smith, G.H., Doerblom, L.A., Sohl-Dickstein, J.N., Wadsworth, M.V., "Athena Microscopic Imager Investigation", Journal Geophysical Research, Vol. 108(E12), 8065, (2003).

[3] Reynolds, R. O., Crowe, D. G., Fernandes, M., "Design of an Active Focus System for a Mars-bound Robotic Arm Camera", Optomechanical Design and Precision Instruments, SPIE Vol. 3132, pg. 78-85, (1997).

[4] Smith, P., Keller, H.U. "The Robotic Arm Camera for Mars Surveyor 2001", Workshop on Mars 2001.

[5] Thomas, N.,.F. Hviid, F., Keller, H.U., Markiewicz, W.J., Blümchen, T., Basilevsky, A.T., Smith, P.H., Tanner, R., Oquest, C., Reynolds, R., Josset., J. –L., Beauvivre, S., Hofmann, B., Rüffer, P., Pillinger8, C.T., Sims, M. R., Pullan, D., and Whitehead., S., "The Microscope for the Beagle 2 Lander on ESA's Mars Express", 6th Interntl. Conf. Mars 2003 #3015.

[6] Dreyer, C.B., Mungas, G.S., Thanh, P., and Radziszewski, J.G., "Study of Sub-mJ-Excited Laser Induced Plasma Combined with Raman Spectroscopy under Mars Atmosphere-Simulated Conditions" Spectrochimica Acta B, Vol. 62 (19), Dec. 2007.

[7] Mungas, G. "Temporally and Spatially Integrated Elemental Analysis Algorithm for Low Pressure Micro-LIBS Measurements". Applied Optics, Vol. 94, (19), July 2007.

[8] Mungas, G., Sepulveda, C., Johnson, K., Pelletier, M., La Baw, C., Boynton, J., Anderson, M., "Raman/CHAMP Instrument for Lunar In-situ Resource Prospecting", IEEEAC#1554 (2006).

[9] Wang, A., Haskin, L. A., Lane, A. L., Wdowiak, T. J., Squyres, S. W., Wilson, R., J., Hovlan, L. E., Manatt, K. S., Raouf, N., Smith, C. D., "Development of the Mars Microbeam Raman Spectrometer", Journal of Geophysical Research, Vol. 108, No. E1, 5005, doi:10.1029/2002JE001902, (2003).

[10] Dreyer, C.B., and Mungas, G.S., "Obscuration of optical transmission due to laser deposited material during micro-LIBS interrogation of a rock surface", Seventh International Conference on Mars #3382 (2007).

[11] Ralchenko, Y., Kramida, A.E., Reader, J., and NIST ASD Team. NIST Atomic Spectra Database (version 3.1.5), [Online]. Available: http://physics.nist.gov/asd3 [2008, July 13]. National Institute of Standards and Technology, Gaithersburg, MD.

[12] Technical Information "Ti-36 Fluorescence of Optical Glass", http://www.schott.com/optics_devices/english/download/index.html, SCHOTT AG (2004).